

Comparison of elevation and remote sensing derived products as auxiliary data for climate surface interpolation

Otto Alvarez,^a Qinghua Guo,^{a,b*} Robert C Klinger,^c Wenkai Li^a and Paul Doherty^a

^a School of Engineering, Sierra Nevada Research Institute, University of California at Merced, CA, USA

^b State Key Laboratory of Vegetation and Environmental Change, Institute of Botany, Chinese Academy of Sciences, Beijing, China

^c USGS, Western Ecological Research Center, Yosemite Field Station, Bishop, CA, USA

ABSTRACT: Climate models may be limited in their inferential use if they cannot be locally validated or do not account for spatial uncertainty. Much of the focus has gone into determining which interpolation method is best suited for creating gridded climate surfaces, which often a covariate such as elevation (Digital Elevation Model, DEM) is used to improve the interpolation accuracy. One key area where little research has addressed is in determining which covariate best improves the accuracy in the interpolation. In this study, a comprehensive evaluation was carried out in determining which covariates were most suitable for interpolating climatic variables (e.g. precipitation, mean temperature, minimum temperature, and maximum temperature). We compiled data for each climate variable from 1950 to 1999 from approximately 500 weather stations across the Western United States (32° to 49° latitude and –124.7° to –112.9° longitude). In addition, we examined the uncertainty of the interpolated climate surface. Specifically, Thin Plate Spline (TPS) was used as the interpolation method since it is one of the most popular interpolation techniques to generate climate surfaces. We considered several covariates, including DEM, slope, distance to coast (Euclidean distance), aspect, solar potential, radar, and two Normalized Difference Vegetation Index (NDVI) products derived from Advanced Very High Resolution Radiometer (AVHRR) and Moderate Resolution Imaging Spectroradiometer (MODIS). A tenfold cross-validation was applied to determine the uncertainty of the interpolation based on each covariate. In general, the leading covariate for precipitation was radar, while DEM was the leading covariate for maximum, mean, and minimum temperatures. A comparison to other products such as PRISM and WorldClim showed strong agreement across large geographic areas but climate surfaces generated in this study (ClimSurf) had greater variability at high elevation regions, such as in the Sierra Nevada Mountains.

KEY WORDS climate surfaces; spatial interpolation; temperature; precipitation; Thin Plate Spline

Received 14 May 2012; Revised 30 August 2013; Accepted 3 September 2013

1. Introduction

Historic and localized weather data are used by climatologists to indicate climate patterns in the past and to make predictions for the future. Normally, the weather station data are sparsely distributed and could be considered as point data. In order to generate wall-to-wall gridded climate surfaces, an interpolation method is needed. Interpolation is a spatial analysis method using points in geographical (e.g. weather stations) and temporal space to predict climate variables in areas where there is no weather observation data (Daly *et al.*, 2002; New *et al.*, 2002; Hijmans *et al.*, 2005; Mbogga *et al.*, 2009). The products from these analyses are known as climate surfaces, and over the last decade they have been increasingly used in a wide range of studies, including ecology, hydrology, fire modelling, and water resources (Bonan *et al.*, 2003; Kalnay and Cai, 2003; Sheffield *et al.*, 2004; Guo *et al.*, 2005; Chen *et al.*, 2007; Trabucco *et al.*, 2008;

Loarie *et al.*, 2009; Mbogga *et al.*, 2009; Thornton *et al.*, 2009). Despite their wide use, there is a need for finer spatial and temporal resolution surfaces to make meaningful inferences at regional and monthly scales (Heikkinen *et al.*, 2006). Temporal resolution is important for relating ecological responses to climate change, especially those associated with population dynamics (birth, death, and migration) of species whose lifespan and fecundity period varies from hours to decades (Walther *et al.*, 2002). With regard to spatial resolution, recent climate surface development has focused on incorporating a high number of weather station data points, but have not fully accounted for the effect of spatial distribution on the validity and interpretation of their models (Thornton *et al.*, 1997; New *et al.*, 1999, 2002; Daly *et al.*, 2000; Maurer *et al.*, 2002; Hijmans *et al.*, 2005; Allan and Ansell, 2006). In this article, we demonstrate how incorporating spatially dependent covariates can lead to more accurate climate surfaces. Specifically, the interpolation method we use is Thin Plate Spline (TPS) with covariates from remote sensing and Digital Elevation Model (DEM) derived products.

* Correspondence to: Q. Guo, School of Engineering, Sierra Nevada Research Institute, University of California at Merced, CA 95343, USA. E-mail: qguo@ucmerced.edu

In climatology, much of the effort has been focused on identifying appropriate weather data interpolation methods. For example, some commonly used methods include TPS, Kriging, and Artificial Neural Networks (ANN) (Hong *et al.*, 2005; Dibike and Coulibaly, 2006; Hancock and Hutchinson, 2006; Stahl *et al.*, 2006; Hofstra *et al.*, 2008). Among those methods, TPS (Hutchinson and Gessler, 1994) is considered as one of the best methods because it is computationally efficient and allows the use of multiple covariates that can improve interpolation accuracy (Wood, 2003). For example, WorldClim, which is one of the most popular climate surfaces because it is global in extent with a spatial resolution of 1 km² and contains four variables (precipitation, mean temperature, minimum temperature, and maximum temperature), was developed using TPS as the interpolation method (Hijmans *et al.*, 2005).

A DEM has been the covariate most frequently used in the development of climate surfaces. However, there has been little evaluation of additional covariates to complement DEM (Diodato, 2005; Daly, 2006). Due to the advances of remote sensing, GIS, and GPS technology, there are a wide range of spatially explicit data available as covariates that could be used to improve interpolation accuracy. Although previous research has suggested that adding such covariates could improve interpolation results, few studies have comprehensively examined the use of other elevation and remote sensing derived products for climate data interpolation (Hijmans *et al.*, 2005). Moreover, lessons learned from geographic information science (GIScience) reiterate the importance of accounting for spatial uncertainty and unequal distribution during interpolation because some relationships between variables vary spatially (Fotheringham *et al.*, 1998). Thus, in order to select the covariates, the product has to meet at least two basic criteria: (1) the data exist wall-to-wall in the study area and (2) fine spatial resolutions (e.g. 1 km²) for most climate products.

The goal of this study was to evaluate the usefulness of including a range of covariates for climate interpolation. On the basis of our understanding of climate factors and the spatial distribution of those factors, we compared the use of DEM and other remote sensing derived products to determine which of these covariates resulted in the greatest improvement in interpolation accuracy. Rather than determining which interpolation method was best or creating a rich collection of weather station information, we focused on investigating what covariate(s) were best suited for particular climatic variables. We explain how we maintained quality control on the observational data, which observation data were used, and how we processed the data that were used as covariates for the interpolation. We then tested our method for different climate variables, precipitation, minimum temperature, maximum temperature, and mean temperature, for the Western United States at monthly and yearly (ranging from 1950 to 1999) temporal resolutions at a spatial resolution of 1 km². Finally, we provided a comparison

to other widely used climate surfaces (i.e. WorldClim (Hijmans *et al.*, 2005) and PRISM (Daly *et al.*, 2002)).

2. Data and methodology

2.1. Study area

We defined the spatial extent of our study (what we refer to hereon as the 'Western US') as the area encompassing the conterminous United States (Figure 1), with a geographic extent of 32° to 49° latitude and -124.7° to -112.9° longitude and area of 1 710 000 square kilometres. It fully covers California, Oregon, Washington, Nevada, and partially covers Idaho (80%), Montana (15%), Utah (10%), and Arizona (10%). The Western US is considered one of the most culturally and ecologically important regions in the world, containing roughly 350 wilderness areas, 20 national parks, and 70 national forests. California in particular is recognized as having relatively high levels of endemism and is also one of only five areas in the world with a Mediterranean climate, which is characterized by warm to hot, dry summers and mild to cool, wet winters (Cowling *et al.*, 2009; Damschen *et al.*, 2010; Mandelik *et al.*, 2010).

2.2. Weather station data and quality control

Weather station data were obtained from the Food and Agriculture Organization FAOclim2.0 (FAO, 2001) and the Global Historical Climate Network Dataset (GHCN) version 2 (Peterson and Vose, 1997). We focused on the time period from 1950 to 1999 and obtained data from 552 stations on precipitation, 357 stations for maximum temperature, 381 stations for minimum temperature, and 415 stations for mean temperature (Figure 1). The time period of 1950 to 1999 was selected since a comparison with other climate surfaces will be performed.

The data were manually checked station by station. For temperature we graphed each station's yearly and monthly means for all of the years available and determined if there were any outliers by visual inspection. For precipitation, we detected outliers with a spatial outlier test, which included the precipitation information from the surrounding weather stations (within 250 km²). Afterwards, we determined if the stations information was correct by comparing the latitude and longitude to its country/city and by comparing the given elevation value to that obtained from the USGS DEM layer.

Most of the errors that were removed or corrected from stations were caused by incorrect units, equipment malfunction, and/or human error. Most of the errors were obvious and easily identified and corrected (e.g. where longitude and latitude for the station were swapped). These situations were generally apparent from the weather station data being markedly different from neighbouring stations. Other weather stations had values that made sense for a period of time, but then appeared to have a multiplier. This was due to the fact that the units for the weather station were changed. Most of the weather

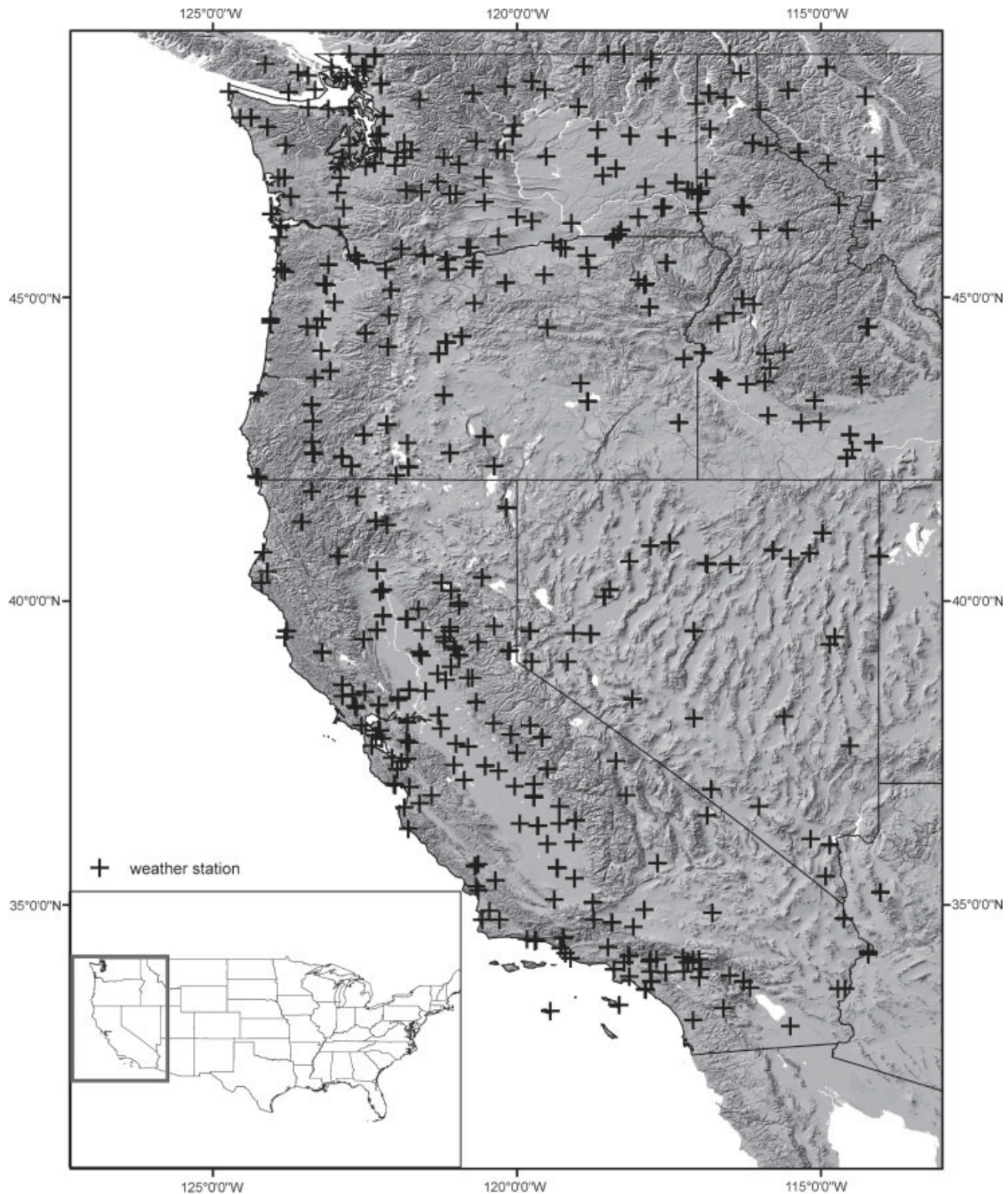


Figure 1. Study area is about 1 710 000 km², ranging from 49° to 32° latitude and -124.7° to -112.9° longitude. It includes California, Oregon, Washington, Nevada, Idaho, Montana, Utah, and Arizona. Weather Station localities for all four climatic variables (precipitation, maximum temperature, minimum temperature, and maximum temperature) ranging from 1950 to 1999. A total of 552 stations for precipitation, 337 stations for maximum temperature, 381 for minimum temperature, and 415 stations for mean temperature.

stations for our study area also reported elevation, so we were able to cross check the recorded elevation with our DEM layer to make sure that the weather station was not at the wrong location. After removing/correcting the weather station data we ended up with 281 904 records for precipitation, 225 128 records for mean temperature, 201 024 records for maximum temperature, and 212 690 records for minimum temperature.

2.3. Remote sensing data

Multiple remote sensing data were obtained from various sources and data acquisition processes (in most cases with resolution of 1 km²):

1. Digital Elevation Model (DEM) was obtained from the Shuttle Radar Topography Mission (SRTM) at 1 km² spatial resolution (Farr *et al.*, 2007).

2. Slope and aspect were generated with the USGS DEM.
3. Distance to coast was calculated for the centre location of each pixel.
4. Two different NDVI products were used: Moderate Resolution Imaging Spectroradiometer (MODIS) and Advanced Very High Resolution Radiometer (AVHRR) (Townshend *et al.*, 1994; Justice *et al.*, 1998). Both products are at 1 km² spatial resolution and are calculated as follows: (Tucker, 1979; Jackson *et al.*, 1983; Tucker *et al.*, 1991)

$$NDVI = \frac{NIR - RED}{NIR + RED} \quad (1)$$

where *NIR* is the near-infrared band and *RED* is the red band. For MODIS the data is available every 16 days from the years of 2000 to 2006. For AVHRR the data is a composite of 10-day periods ranging from April 1992 to May 1996. Both datasets were reduced by first taking the maximum of each month per year (if multiple images exist per month), then taking the average of all the years to obtain a monthly average for its corresponding time period (Eklundh, 1995).

5. Solar potential was generated using the hemispherical viewshed algorithm:

$$Point\ radiation = direct_{total} + diffuse_{total} \quad (2)$$

where *direct_{total}* and *diffuse_{total}* are the sum of radiation of all sectors (Rich *et al.*, 1994). Using the slope and aspect generated from SRTM DEM data we generated the hourly solar potential for 2010. The output was then averaged per month, leading to a monthly solar potential layer at 1 km² spatial resolution. All calculations were carried out with the ArcGIS solar potential toolbox (ESRI, 2009).

6. Radar rainfall data is calculated from multi-sensor data (radar and rain gauge) by the National Oceanic and Atmospheric Administration (NOAA) National Weather Service (NOAA, 2012). The data ranges from 1997 to 2010 and were reduced to create an average for 1997–2010 with a spatial resolution of approximately 4 km². Because we wanted the resolution of our final monthly products to be 1 km², we used TPS to interpolate the radar data to this scale using DEM as a covariate with a second order polynomial (see Section 4).
7. For precipitation, we used three temperature surfaces: maximum, minimum, and mean model outputs as covariates. The temperature surfaces were generated using TPS with DEM as a covariate.

2.4. Climate interpolation and evaluation

To generate climate surfaces, we used TPS in the package ‘Fields’ version 6.3 in R version 2.7.1 (Furrer *et al.*, 2011). TPS aims to derive coherent signals and remove noise from an interpolation (Wahba and Wendelberger, 1980; Wahba, 1990), and was first applied in climatology

by Hutchinson *et al.* (Hutchinson and Gessler, 1994; Hutchinson, 1995). The following equation is for TPS for two independent position covariates and extra covariates:

$$q_i = f \left(x_i, y_i + \sum_{j=1}^p \beta_j \psi_{ij} + \epsilon_i \quad (i = 1, \dots, n) \right) \quad (3)$$

and the smoothing function $f(x_i, y_i)$ and β_i are estimated by minimizing:

$$\sum_{i=1}^n \left[\frac{q_i - f(x_i, y_i) - \sum_{j=1}^p \beta_j \psi_{ij}}{d_i} \right]^2 + \lambda J_m(f) \quad (4)$$

where $f(x_i, y_i)$ is the unknown smooth function, β_i is a set of unknown parameters, x_i, y_i, ψ_{ij} are the independent variables, ϵ_i is the independent random errors with zero mean and variance ($d_i \sigma^2$), d_i are the known weights, $J_m(f)$ is a measure of the smoothness of f defined in terms of m th order derivatives of f , and λ is the smoothing parameter (Hutchinson and Gessler, 1994; Hutchinson, 1995).

To evaluate which covariate produced the lowest uncertainty for each climatic variable, a tenfold cross-validation approach was used (Kohavi, 1995; Hijmans *et al.*, 2005). The climatic data are first divided randomly into 10 sub-samples and then TPS is run on 9 of 10 sub-samples, retaining one sub-sample to validate the model. We repeated the process ten times, guaranteeing that all of the points are used for both training and validation. The model accuracy was then determined by the Root Mean Square Error (RMSE).

$$RMSE = \sqrt{\frac{\sum_{i=1}^n (x_i^p - x_i^r)^2}{n}} \quad (5)$$

where x_i^p and x_i^r are the model prediction and observed value for point i , and n is the total number of points. This is calculated monthly, having a total of 10 (runs cross-validation) by 12 (months) = 120 runs per climatic variable and covariate. After selecting the best covariate(s), all the points are then used to create the monthly average from 1950 to 1999 climate surfaces at a spatial resolution of 1 km². Then, using the same parameters, a monthly climate surface was generated for each year, creating 50 (years) × 12 (months) = 600 climate surfaces per climatic variable.

In lieu of just ‘blindly’ separating the study area, we calculated the uncertainty for precipitation based on ecoregional and DEM classifications. We used the four level I ecoregional classifications from the United States Environmental Protection Agency that fell in our study area: (1) Marine west coast forest, (2) Mediterranean California, (3) North American deserts, and (4) Northwestern

forested mountains (EPA, 2012). For the DEM classification we selected four classes using natural breaks: (1) <550 m, (2) 550–1174 m, (3) 1175–1822 m, (4) >1822 m. Each weather station was then grouped based on its location and the total annual uncertainty for all weather stations in that region/class for precipitation was calculated.

To compare our climate surfaces with PRISM and WorldClim, we first processed all three datasets to the same spatial resolution. We reduced the spatial resolution of our product (ClimSurf) and WorldClim to match PRISM (4 km²) by spatial upscaling, then reduced the temporal resolution to match WorldClim by creating an average from 1950 to 1999. Finally, the total annual precipitation (mm) was calculated. Temperature variables were not included in the comparison since the products would covary tightly with DEM, and we found the temperature variables were very similar among three products.

3. Results

3.1. Covariate and uncertainty

For all three temperatures, DEM alone had the lowest uncertainty value across all possible combinations. In most cases, when DEM was added with another covariate it also produced a relatively low uncertainty value; the only exception was the combination of DEM and slope,

which results in a very high uncertainty. For maximum and minimum temperature the combination of DEM and distance to coast had a lower uncertainty than DEM alone (Table 1). Adding slope to any other covariate for both mean and minimum temperature produced a high uncertainty value (Tables 2–4). The uncertainty for radar as a covariate for the three temperatures was very close to the uncertainty value for DEM, distance to coast, and both NDVI measures, which also had low uncertainty values. The best covariate for precipitation was radar, with ~20% less uncertainty than DEM (Table 1). We note that the pattern of low uncertainty for temperature that we observed when DEM and any other covariate were added to the interpolation was mirrored when adding any covariate with DEM for precipitation. The use of one of the three temperature variables as a covariate for precipitation produced better results than the use of DEM. Adding multiple covariates did not necessarily reduce uncertainty; in most cases these covariates actually increased the uncertainty for all four climate variables.

3.2. Errors and comparison

The patterns for all three climate surfaces were similar (Figure 2), with most of the differences occurring in places with higher elevation, such as the Sierra Nevada Mountains. This disagreement is likely due to three facts: (1) different weather station data, (2) different interpolation methods, and (3) different covariates that were used

Table 1. The uncertainty (RMSE) calculated from the tenfold cross-validation for annual precipitation (mm) for each 1–2 possible covariate combination.

	DEM	Radar	Slope	Solar P.	Aspect	AVHRR NDVI	MODIS NDVI	Tmax	Tmean	Tmin	Distance to coast
DEM	189.56										
Radar	162.23	148.06									
Slope	>200	>200	195.01								
Solar P.	>200	184.88	>200	>200							
Aspect	>200	171.69	>200	>200	>200						
AVHRR NDVI	>200	172.53	>200	>200	>200	>200					
MODIS NDVI	>200	164.99	>200	>200	>200	>200	>200				
Tmax	196.69	162.13	>200	>200	>200	>200	>200	187.51			
Tmean	194.34	167.55	>200	>200	>200	>200	>200	>200	187.11		
Tmin	195.68	167.65	>200	>200	>200	>200	>200	227.64	197.64	199.45	192.37
Distance to coast	184.38	183.06	>200	>200	>200	>200	238.19	187.01	>200	188.19	180.18

Table 2. The uncertainty (RMSE) calculated from the tenfold cross-validation for annual mean temperature (Kelvin) for each 1–2 possible covariate combination.

	DEM	Radar	Slope	Solar P.	Aspect	AVHRR NDVI	MODIS NDVI	Distance to coast
DEM	18.66							
Radar	20.25	19.91						
Slope	>30	>30	19.98					
Solar P.	>30	>30	>30	20.35				
Aspect	20.63	26.76	>30	>30	21.13			
AVHRR NDVI	19.58	21.36	>30	>30	23.70	20.12		
MODIS NDVI	20.17	22.44	>30	>30	>30	>30	21.22	
Distance to coast	21.41	23.88	27.68	22.55	29.26	24.92	25.96	20.15

Table 3. The uncertainty (RMSE) calculated from the tenfold cross-validation for annual maximum temperature (Kelvin) for each 1–2 possible covariate combination.

	DEM	Radar	Slope	Solar P.	Aspect	AVHRR NDVI	MODIS NDVI	Distance to coast
DEM	21.02							
Radar	21.81	23.40						
Slope	22.48	25.17	24.07					
Solar P.	21.34	22.30	23.29	27.15				
Aspect	21.84	25.15	26.69	23.61	25.09			
AVHRR NDVI	21.49	24.02	26.36	22.28	25.69	23.83		
MODIS NDVI	21.97	24.92	26.76	23.45	25.84	25.16	24.63	
Distance to coast	20.96	23.21	38.85	24.15	23.85	22.90	23.69	22.59

Table 4. The uncertainty (RMSE) calculated from the tenfold cross-validation for annual minimum temperature (Kelvin) for each 1–2 possible covariate combination.

	DEM	Radar	Slope	Solar P.	Aspect	AVHRR NDVI	MODIS NDVI	Distance to coast
DEM	21.30							
Radar	22.02	22.50						
Slope	>30	>30	22.29					
Solar P.	21.71	24.65	>30	22.95				
Aspect	22.82	25.84	>30	25.35	24.38			
AVHRR NDVI	23.70	24.81	>30	25.28	26.16	23.62		
MODIS NDVI	22.29	24.89	>30	24.99	27.08	25.83	23.81	
Distance to coast	20.84	22.08	25.31	25.47	25.41	23.59	23.26	21.32

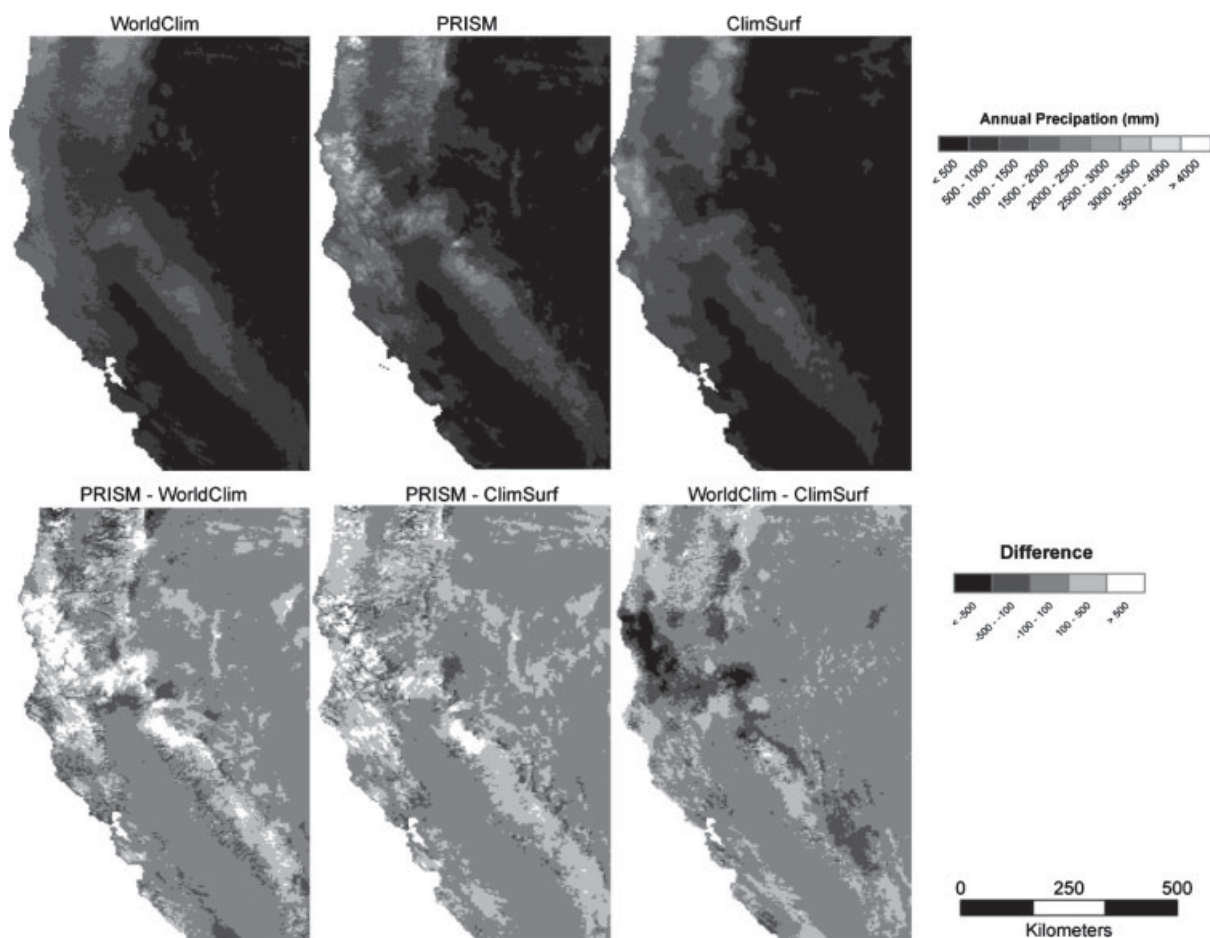


Figure 2. (Top row) Comparison of PRISM, WorldClim, and ClimSurf for total annual precipitation (mm) and bitwise difference between all three climate surface products (bottom row). Data was rescaled to match the coarser spatial and temporal resolution which was 4 km² and average of 1950–1999.

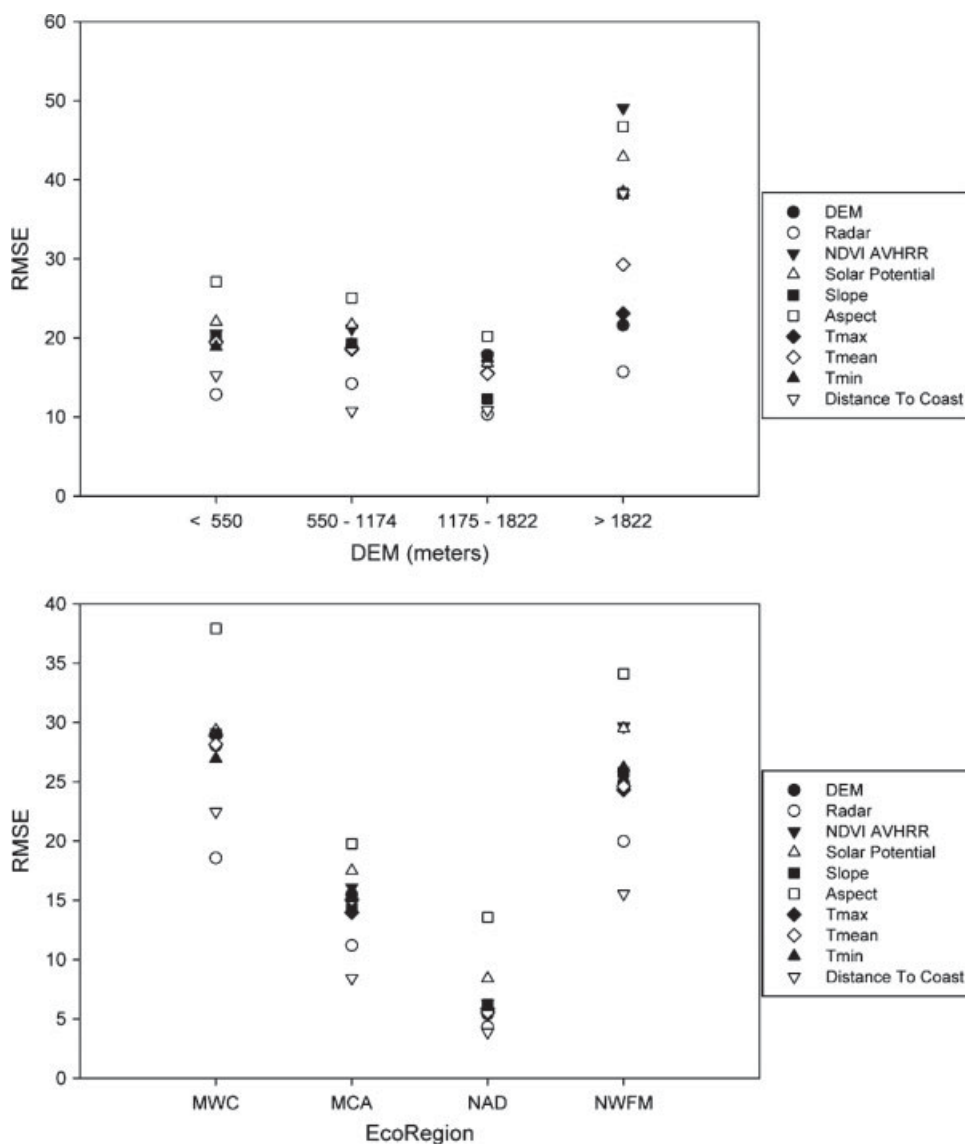


Figure 3. The uncertainty for total annual precipitation (mm), for multiple covariates (TOP) by dividing elevation into four different classes: (1) <550 (3062 points), (2) 550–1174 (5998 points), (3) 1175–1822 (936 points), (4) >1822 (168 points) (BOTTOM) by ecoregion, four classes are in located in our study area, (MWC) Marine west coast forest (752 points), (MCA) Mediterranean California (1307 points), (NAD) North American deserts (2027 points), (NWFM) Northwestern forested mountains (1864 points).

in the interpolation. For example, ClimSurf only used two sources of weather station data, whereas the other surfaces used a few more such as WMO (see Section 2).

3.3. Precipitation by elevation and ecoregion classes

Figure 3 shows the uncertainty for precipitation surface separated by elevation and ecoregion classes. In general, radar and distance to coast were the two covariates that produced the lowest uncertainty. The analysis indicated that aspect yielded the greatest uncertainty regardless of the elevation class. The only class in which aspect did not give the greatest uncertainty was in elevation class 4 (above 1833 m), where NDVI derived from AVHRR was the highest. In the Marine west coast forest ecoregion, there was a cluster of covariates that yielded almost identical uncertainties, but uncertainties by these covariates were approximately 40% higher than radar.

For the elevation classes we observed the same pattern as for the Marine west coast forest ecoregion, a cluster of covariates giving uncertainties about 40% higher than radar. For class 3 (1175 to 1822 m) we observed that slope performed better than DEM and very close to radar. The class that was most interesting was class 4, the highest elevation class (more than 1822 m). All the points were scattered over the range of 15–50 mm of uncertainty, which is most likely a result of fewer observation points in high elevation areas.

4. Discussion and conclusion

4.1. Uncertainty

Uncertainty in precipitation values was not minimized using DEM alone. Interestingly, NDVI resulted in a

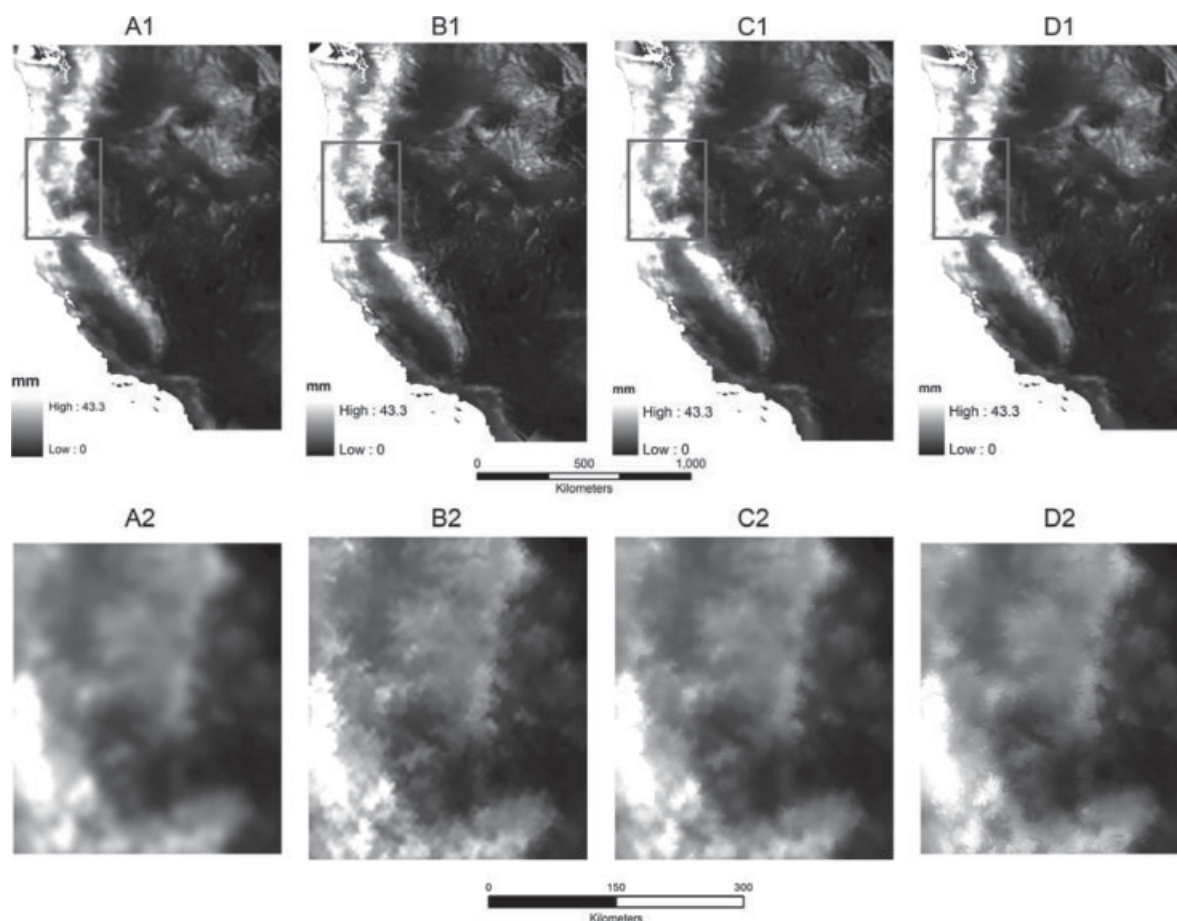


Figure 4. Comparison of interpolating radar data from 4 to 1 km² using multiple algorithms (A, Universal Kriging; B, Regular Spline; C, Inverse Distance Weighted; D, Thin Plate Spline) for the month of January.

higher uncertainty than DEM for precipitation. We did not expect these results since NDVI, vegetation productivity, and precipitation usually have strong correlations with each other (Ichii *et al.*, 2002). One possible reason is that the NDVI derived from remote sensing data has large uncertainty, which will propagate into the interpolated precipitation surface. We found that while both MODIS and AVHRR were good covariates, they did not produce lower uncertainty than DEM. This required additional data, in particular radar. However, one problem with using radar data (as mentioned in Section 2) was the coarse spatial resolution (4 km²). In our preliminary analyses multiple interpolation algorithms were run including Kriging, IDW, Regular Spline, and TPS. On visual inspection we noticed that the new interpolated radar surface did not contain much detail. On the basis of previous processing attempts with different covariates, we found that, in most cases, adding multiple covariates increased the total uncertainty. We then ran the radar 4 km² data with TPS and DEM as a covariate (Figure 4). By adding DEM as a covariate to refine the radar resolution, we were indirectly including two covariates in interpolating precipitation, and hence were able to decrease the uncertainty in precipitation.

Although radar did not always produce the lowest uncertainty for precipitation in different elevation and

ecoregion classes, it did have the lowest overall uncertainty value among the covariates. This is an intrinsic relationship as radar is essentially a measurement of liquid water in the atmosphere. Radar is a known proxy for precipitation and hence is a strong candidate for covariation. The difference from the lowest (radar) to the highest (usually aspect) uncertainty varied from 5% to as high as 60%. As shown in Figure 5, we observed that radar covaried with the observed weather station data more closely than DEM, though both covariates had a strong correlation.

When precipitation was stratified by month the results indicated that during wet months (November through February) using radar as a covariate decreased the uncertainty by as much as 33% relative to using DEM (Figure 6). During warmer, drier months the contrast was smaller, but radar still had the lowest uncertainty among the covariates. Aspect, NDVI and solar potential yielded the greatest uncertainty for each month, with aspect yielding as high as double and solar potential as high as 80% greater than radar during the wet season. The uncertainty for these covariates was reduced during the warmer months, but even so, they were low-ranking variables.

It should also be noted that adding multiple covariates could increase rather than decrease the uncertainty in

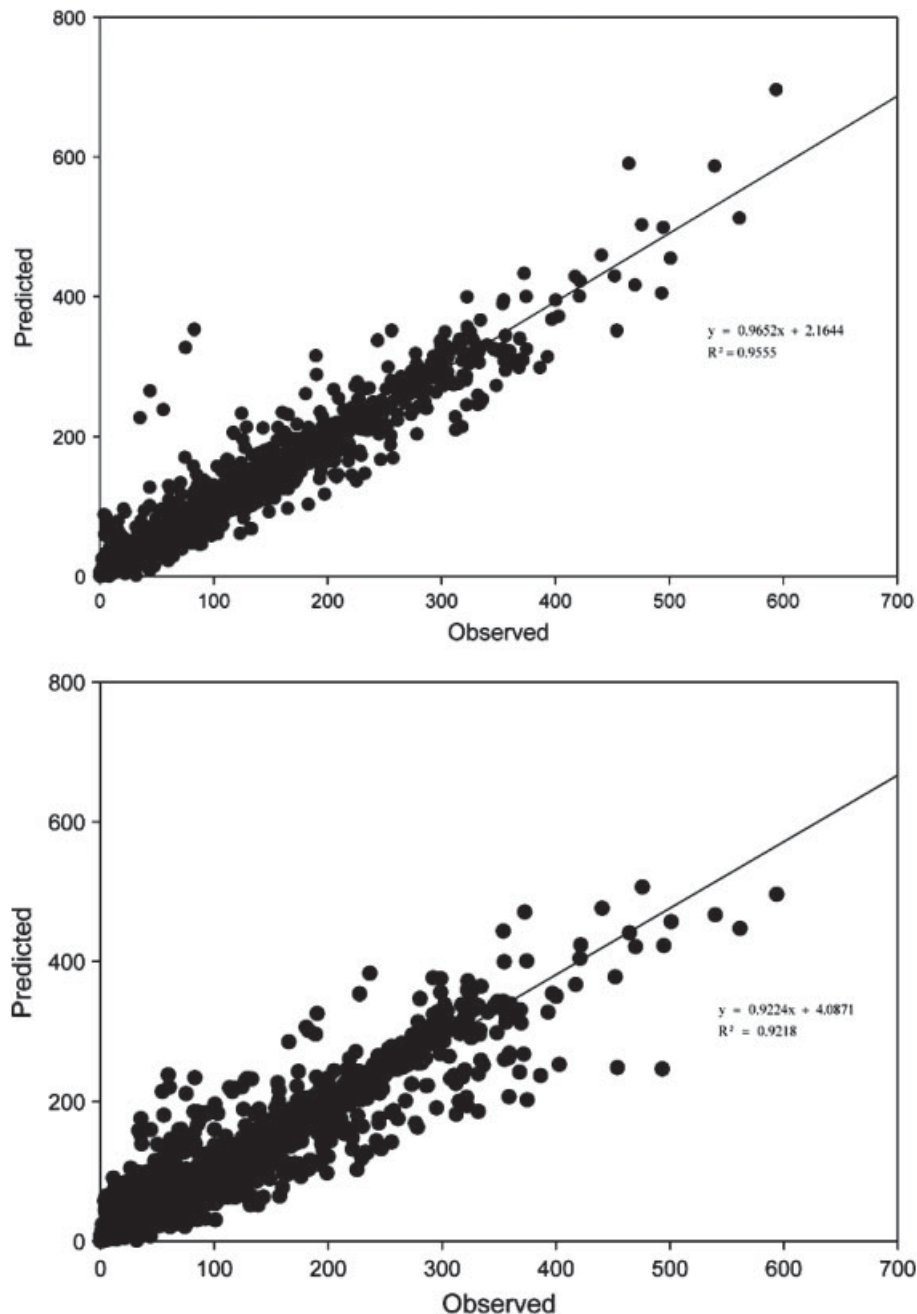


Figure 5. Output of the tenfold cross-validation (RMSE): *x*-axis, observer station data; *y*-axis, interpolated model prediction for precipitation (mm). (Top) Radar as a covariate (bottom) DEM as a covariate.

most cases, for all four climate variables. This can possibly be due to error propagation. Adding more covariates will add more sources of errors, which will propagate into the final product. Another possible reason is over-fitting. For the same sample size, adding more covariates can increase the risk of over-fitting. If we have more observation data, then the problem of over-fitting can be reduced.

4.2. Improvements and conclusion

As with any climate surface, we experienced limitations. The main one this was the lack of data in high elevation regions, and not surprisingly was where the

greatest uncertainties were found. Note though that adding weather station data does not always improve climate surfaces. For instance, if the data are located in regions of existing high station density then it is unlikely much unique information would be gained from its inclusion. The second limitation was that, although TPS is considered one of the best interpolation methods (Hong *et al.*, 2005; Dibike and Coulibaly, 2006; Hancock and Hutchinson, 2006; Stahl *et al.*, 2006; Hofstra *et al.*, 2008), we did not test it against other interpolation methods, such as ANN or Kriging.

There are many future directions for improving climate surfaces other than simply adding more weather station

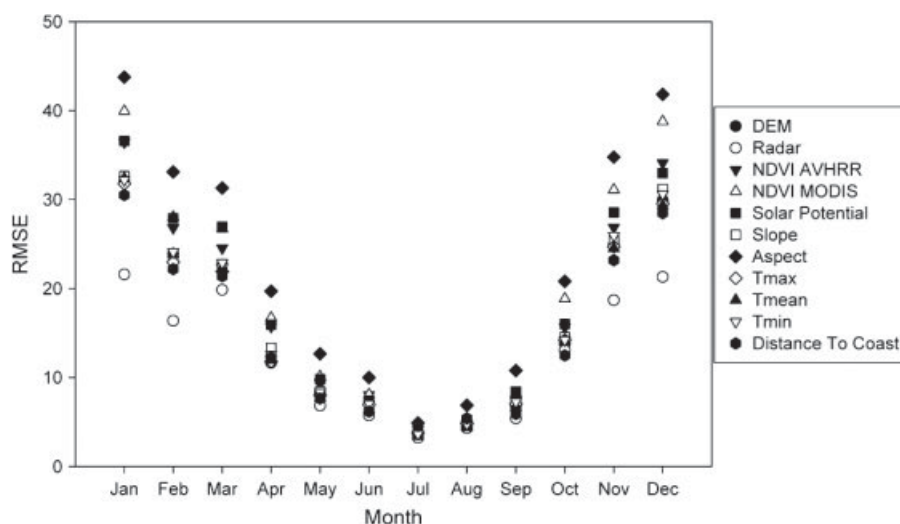


Figure 6. The uncertainty (y-axis) of total monthly precipitation (mm) for each covariate, display in monthly time-steps.

data or generating a set of global climate surfaces. A key objective of this study was to probe more effective approaches rather than simply using traditional covariates (DEM) and explore other potential sources of co-varying environmental influences. We did not use other potential remote sensing data that might have an influence on the climatic variables, such as snow cover. However, indirectly adding multiple covariates as we did with radar may often be an effective approach in reducing uncertainty.

In conclusion, significant work has been carried out to determine what covariate is best suited for each climate variable. We have shown that there are better products which will help reduce the uncertainty, however, we know that there might be other products that might as well be better suited. We made a visual comparison with other well known products to visually show the differences and between those products.

Acknowledgements

This study is supported by “973” Program (2013 CB956604), the National Science Foundation of China (31270563), and USGS National Climate Change and Wildlife Science Center. We thank the reviewer comments that strengthened this manuscript.

References

- Allan R, Ansell T. 2006. A new globally complete monthly historical gridded mean sea level pressure dataset (hadslp2): 1850–2004. *J. Climate* **19**(22): 5816–5842.
- Bonan GB, Levis S, Storch S, Vertenstein M, Oleson KW. 2003. A dynamic global vegetation model for use with climate models: concepts and description of simulated vegetation dynamics. *Glob. Chang. Biol.* **9**(11): 1543–1566.
- Chen H, Guo S, Xu C-Y, Singh VP. 2007. Historical temporal trends of hydro-climatic variables and runoff response to climate variability and their relevance in water resource management in the Hanjiang basin. *J. Hydrol.* **344**(3–4): 171–184.

- Cowling RM, Proches S, Partridge TC. 2009. Explaining the uniqueness of the cape flora: incorporating geomorphic evolution as a factor for explaining its diversification. *Mol. Phylogenet. Evol.* **51**(1): 64–74.
- Daly C. 2006. Guidelines for assessing the suitability of spatial climate data sets. *Int. J. Climatol.* **26**(6): 707–721.
- Daly C, Taylor GH, Gibson WP, Parzybok TW, Johnson GL, Pasteris PA. 2000. High-quality spatial climate data sets for the United States and beyond. *Trans. ASAE* **43**(6): 1957–1962.
- Daly C, Gibson WP, Taylor GH, Johnson GL, Pasteris P. 2002. A knowledge-based approach to the statistical mapping of climate. *Climate Res.* **22**(2): 99–113.
- Damschen EI, Harrison S, Grace JB. 2010. Climate change effects on an endemic-rich edaphic flora: resurveying Robert H. Whittaker’s Siskiyou sites (Oregon, USA). *Ecology* **91**(12): 3609–3619.
- Dibike YB, Coulibaly P. 2006. Temporal neural networks for down-scaling climate variability and extremes. *Neural Netw.* **19**(2): 135–144.
- Diodato N. 2005. The influence of topographic co-variables on the spatial variability of precipitation over small regions of complex terrain. *Int. J. Climatol.* **25**(3): 351–363.
- Eklundh LR. 1995. Noise estimation in NOAA AVHRR maximum-value composite NDVI images. *Int. J. Remote Sens.* **16**(15): 2955–2962.
- EPA. 2012. EPA. Retrieved May 1, 2012. <http://www.epa.gov/wed/pages/ecoregions.htm>.
- ESRI. 2009. *ArcMap 9.3*. ESRI. Redlands, California.
- FAO. 2001. *FAOCLIM 2.0 A World-Wide Agroclimatic Database*. Food and Agriculture Organization of the United Nations.
- Farr TG, Rosen PA, Caro E, Crippen R, Duren R, Hensley S, Kobrick M, Paller M, Rodriguez E, Roth L, Seal D, Shaffer S, Shimada J, Umland J, Werner M, Oskin M, Burbank D, Alsdorf D. 2007. The shuttle radar topography mission. *Rev. Geophys.* **45**(2), DOI: 10.1029/2005RG000183.
- Fotheringham AS, Charlton ME, Brunson C. 1998. Geographically weighted regression: a natural evolution of the expansion method for spatial data analysis. *Environ. Plan. A* **30**(11): 1905–1927.
- Furrer R, Nychka D, Sain S. 2011. *Package ‘fields’*. Retrieved May 1, 2012. <http://cran.rproject.org/web/packages/fields/index.html>.
- Guo QH, Kelly M, Graham CH. 2005. Support vector machines for predicting distribution of sudden oak death in California. *Ecol. Model.* **182**(1): 75–90.
- Hancock PA, Hutchinson MF. 2006. Spatial interpolation of large climate data sets using bivariate thin plate smoothing splines. *Environ. Model. Software* **21**(12): 1684–1694.
- Heikkinen RK, Luoto M, Araujo MB, Virkkala R, Thuiller W, Sykes MT. 2006. Methods and uncertainties in bioclimatic envelope modelling under climate change. *Prog. Phys. Geogr.* **30**(6): 751–777.
- Hijmans RJ, Cameron SE, Parra JL, Jones PG, Jarvis A. 2005. Very high resolution interpolated climate surfaces for global land areas. *Int. J. Climatol.* **25**(15): 1965–1978.

- Hofstra N, Haylock M, New M, Jones P, Frei C. 2008. Comparison of six methods for the interpolation of daily, European climate data. *J. Geophys. Res. Atmos.* **113**: D21.
- Hong Y, Nix HA, Hutchinson MF, Booth TH. 2005. Spatial interpolation of monthly mean climate data for china. *Int. J. Climatol.* **25**(10): 1369–1379.
- Hutchinson MF. 1995. Interpolating Mean Rainfall Using Thin-Plate Smoothing Splines. *Int. J. Geogr. Inf. Syst.* **9**(4): 385–403.
- Hutchinson MF, Gessler PE. 1994. Splines - more than just a smooth interpolator. *Geoderma* **62**(1–3): 45–67.
- Ichii K, Kawabata A, Yamaguchi Y. 2002. Global correlation analysis for NDVI and climatic variables and NDVI trends: 1982–1990. *Int. J. Remote Sens.* **23**(18): 3873–3878.
- Jackson RD, Slater PN, Pinter PJ. 1983. Discrimination of growth and water-stress in wheat by various vegetation indexes through clear and turbid atmospheres. *Remote Sens. Environ.* **13**(3): 187–208.
- Justice CO, Vermote E, Townshend JRG, Defries R, Roy DP, Hall DK, Salomonson VV, Privette JL, Riggs G, Strahler A, Lucht W, Myneni RB, Knyazikhin Y, Running SW, Nemani RR, Wan ZM, Huete AR, van Leeuwen W, Wolfe RE, Giglio L, Muller JP, Lewis P, Barnsley MJ. 1998. The moderate resolution imaging spectroradiometer (MODIS): land remote sensing for global change research. *IEEE Trans. Geosci. Remote Sens.* **36**(4): 1228–1249.
- Kalnay E, Cai M. 2003. Impact of urbanization and land-use change on climate. *Nature* **423**(6939): 528–531.
- Kohavi R. 1995. A study of cross-validation and bootstrap for accuracy estimation and model selection. *Int. Joint Conf. Artif. Intell.* **14**: 1137–1145.
- Loarie SR, Duffy PB, Hamilton H, Asner GP, Field CB, Ackerly DD. 2009. The velocity of climate change. *Nature* **462**(7276): 1052–1111.
- Mandelik Y, Roll U, Fleischer A. 2010. Cost-efficiency of biodiversity indicators for Mediterranean ecosystems and the effects of socio-economic factors. *J. Appl. Ecol.* **47**(6): 1179–1188.
- Maurer EP, Wood AW, Adam JC, Lettenmaier DP, Nijssen B. 2002. A long-term hydrologically based dataset of land surface fluxes and states for the conterminous United States. *J. Climate* **15**(22): 3237–3251.
- Mbogga MS, Hamann A, Wang T. 2009. Historical and projected climate data for natural resource management in western Canada. *Agr. Forest. Meteorol.* **149**(5): 881–890.
- New M, Hulme M, Jones P. 1999. Representing twentieth-century space-time climate variability. Part I: development of a 1961–90 mean monthly terrestrial climatology. *J. Climate* **12**(3): 829–856.
- New M, Lister D, Hulme M, Makin I. 2002. A high-resolution data set of surface climate over global land areas. *Climate Res.* **21**(1): 1–25.
- NOAA. 2012. *Downloading Gridded Rainfall Data*. Retrieved May 1, 2012. <http://water.weather.gov/precip/download.php>.
- Peterson TC, Vose RS. 1997. An overview of the global historical climatology network temperature database. *Bull. Am. Meteorol. Soc.* **78**(12): 2837–2849.
- Rich PM, Dubayah R, Hetrick WA, Saving SC. 1994. Using viewshed models to calculate intercepted solar potential: applications in ecology. *Am. Soc. Photogramm. Remote Sens. Tech. Papers*: 524–529.
- Sheffield J, Ziegler AD, Wood EF, Chen YB. 2004. Correction of the high-latitude rain day anomaly in the NECP-NCAR reanalysis for land surface hydrological modeling. *J. Climate* **17**(19): 3814–3828.
- Stahl K, Moore RD, Floyer JA, Asplin MG, McKendry IG. 2006. Comparison of approaches for spatial interpolation of daily air temperature in a large region with complex topography and highly variable station density. *Agr. Forest. Meteorol.* **139**(3–4): 224–236.
- Thornton PE, Running SW, White MA. 1997. Generating surfaces of daily meteorological variables over large regions of complex terrain. *J. Hydrol.* **190**(3–4): 214–251.
- Thornton PK, Jones PG, Alagarswamy G, Andresen J. 2009. Spatial variation of crop yield response to climate change in east Africa. *Global Environ. Chang.* **19**(1): 54–65.
- Townshend JRG, Justice CO, Skole D, Malingreau JP, Cihlar J, Teillet P, Sadowski F, Ruttenberg S. 1994. The 1 km resolution global data set – needs of the international geosphere biosphere program. *Int. J. Remote Sens.* **15**(17): 3417–3441.
- Trabucco A, Zomer RJ, Bossio DA, van Straaten O, Verchot LV. 2008. Climate change mitigation through afforestation/reforestation: a global analysis of hydrologic impacts with four case studies. *Agr. Ecosyst. Environ.* **126**(1–2): 81–97.
- Tucker CJ. 1979. Red and photographic infrared linear combinations for monitoring vegetation. *Remote Sens. Environ.* **8**(2): 127–150.
- Tucker CJ, Newcomb WW, Los SO, Prince SD. 1991. Mean and inter-year variation of growing-season normalized difference vegetation index for the Sahel 1981–1989. *Int. J. Remote Sens.* **12**(6): 1133–1135.
- Wahba G. 1990. *Spline Models for Observational Data*. Society for Industrial and Applied Mathematics: Philadelphia, PA.
- Wahba G, Wendelberger J. 1980. Some new mathematical-methods for variational objective analysis using splines and cross validation. *Mon. Weather Rev.* **108**(8): 1122–1143.
- Walther GR, Post E, Convey P, Menzel A, Parmesan C, Beebee TJC, Fromentin JM, Hoegh-Guldberg O, Bairlein F. 2002. Ecological responses to recent climate change. *Nature* **416**(6879): 389–395.
- Wood SN. 2003. Thin plate regression splines. *J. Roy. Stat. Soc. Ser. B: Stat. Methodol.* **65**: 95–114.